Research Article

Low Temperature Conductivity in *n*-Type Noncompensated Silicon below Insulator-Metal Transition

A. L. Danilyuk,[1] A. G. Trafimenko,[1] A. K. Fedotov,[2] I. A. Svito,[2] and S. L. Prischepa[1]

[1]*Belarusian State University of Informatics and Radioelectronics, P. Browka 6, 220013 Minsk, Belarus*
[2]*Belarusian State University, Nezalezhnastsi Av. 4, 220030 Minsk, Belarus*

Correspondence should be addressed to S. L. Prischepa; prischepa@bsuir.by

We investigate the transport properties of *n*-type noncompensated silicon below the insulator-metal transition by measuring the electrical and magnetoresistances as a function of temperature T for the interval 2–300 K. Experimental data are analyzed taking into account possible simple activation and hopping mechanisms of the conductivity in the presence of two impurity bands, the upper and lower Hubbard bands (UHB and LHB, resp.). We demonstrate that the charge transport develops with decreasing temperature from the band edge activation (110–300 K) to the simple activation with much less energy associated with the activation motion in the UHB (28–90 K). Then, the Mott-type variable range hopping (VRH) with spin dependent hops occurs (5–20 K). Finally, the VRH in the presence of the hard gap (HG) between LHB and UHB (2–4 K) takes place. We propose the empiric expression for the low T density of states which involves both the UHB and LHB and takes into account the crossover from the HG regime to the Mott-type VRH with increasing temperature. This allows us to fit the low T experimental data with high accuracy.

1. Introduction

Interest in studies of conductivity mechanisms in semiconductor materials, including traditional doped semiconductors near the metal-insulator transition (MIT), does not stop currently [1, 2]. This is due to both the fundamental problems of electron transport in the vicinity of such transition and applied aspects related to the development of highly sensitive sensors of magnetic and electric fields. In particular, it is not yet fully understood mechanisms of low temperature electrical conductivity in doped semiconductors involving multiply charged localized states, mechanisms of positive and negative magnetoresistance (MR), as well as mechanisms of localization and peculiarities of the energy band structures of impurity and localized states. Due to the above the detailed investigation of the conductivity of doped semiconductors near the MIT in a wide temperature range, influence on it the magnetic field is still relevant. Actually, the MIT in three dimensional (3D) system occurs when the Mott criterion $N_c^{1/3} a_B \approx 0.25$ is satisfied, where N_c is the critical concentration of the localized states for the MIT

and a_B is the effective Bohr radius of an insulated defect center [3]. The validity of this criterion was confirmed in various experiments [4–6]. However, some ambiguity in correct understanding of the temperature dependence of the conductivity and MR near the critical concentration of the localized sites still does present. The main reason for this is related to the competition between various types of hopping conductivity, mechanisms of weak localization, percolation and metallic and/or impurity bands (Hubbard bands) conductivity. Therefore, a series of crossovers could be observed between different types of conductivity in a wide temperature range. This inevitably leads to the need for their very careful consideration during the processing of the experimental data. In particular, with decreasing temperature, the crossover from band edge activation (ϵ_1) to hopping (ϵ_3) conductivity is observed in doped semiconductors [6].

Hopping is one of the most likely mechanisms that determines the overall conductivity on the insulating side of the MIT. Among various types of hops, the variable range hopping (VRH) is one of the most relevant. The VRH mechanism, in turn, could be classified as the Mott

mechanism, for which the density of states (DOS) on the Fermi level is constant, $g(E_F) = $ const [3] and the Efros-Shklovskii (ES) mechanism, which implies the soft Coulomb gap (CG), $g(E) \sim |E - E_F|^2$ [7, 8]. From a practical point of view, at a constant T, the Mott-type VRH occurs when the doping concentration N_d is far less than the N_c value, $N_d < 0.5 N_c$, and one can neglect the Coulomb interaction [9]. The ES mechanism, in turn, dominates when $N_d > 0.6 N_c$ and the CG has to be taken into account [10, 11]. From the literature a few models of crossovers between the Mott and ES hopping are known quite [12–14].

The temperature dependence of the resistivity for both mechanisms is described by the well-known expression

$$\rho(T) = \rho_0 \exp\left(\frac{T_h}{T}\right)^p, \tag{1}$$

where ρ_0 is the preexponential factor and T_h and p are the characteristic temperature and exponent, respectively. Last two quantities depend on the mechanism of hopping. In particular, for 3D systems and for the Mott mechanism, the exponent $p = 1/4$, while for the ES VRH $p = 1/2$ [3, 6]. The exponent p can be obtained from the experiment.

Actually, the concept of hopping between disorder-induced localized electronic states near the MIT is a universal feature of disordered Mott systems. In particular, it was successfully applied to describe transport in amorphous/nanocrystalline silicon hybrids [15], semiconductor nanocrystals [16], ruthenate [17], carbon nanotube fibers [18], as well as transport of single (few) donors in a silicon nanoscale transistor [19, 20]. Known models of crossover between different types of VRH are characterized by two different approaches to the calculation of the exponent p from (1). The first approach is based on the analysis of the percolation problem [12, 13, 21], while the second deals with the optimization of the exponent p using the interpolation expression for the DOS [14, 22, 23].

In general, the percolation approach can be applied when the spatial correlation length for the random potential is much larger than the phase coherence length [24, 25]. This is a very powerful tool for the description of charge transport in disordered systems with localized states, which occurs due to the electron hops from one site to another [26, 27]. It should be noted that the percolation theory was applied to explain the properties not only of doped semiconductors, but also granular metals [28], manganese oxides [29], quantum Hall plateau transistors [30], high-T_c cuprates [31], and so forth. Moreover, the percolation phase was directly observed in vanadium dioxide close to the Mott transition by means of nanoscale X-ray imaging [32].

The second approach is less stringent and leads to a noticeable overestimation of the width of the crossover region. General description of the crossover from the Mott to ES VRH on the basis of rather complex multivariable integral equation, which cannot be solved analytically and needs rather difficult numerical analysis, was proposed in [13]. In [14, 22, 23] the procedure based on the optimization of the exponent in the expression for the hopping probability and using the interpolation expression for the DOS, $g(E) \sim$

$|E - E_F|^n$ (here n is integer which is equal to 0 for the Mott mechanism and to 2 for the ES VRH), has been proposed. This approach leads to quite simple analytical expressions but, as we mentioned above, is less stringent than the percolation task.

In addition to the crossover from the Mott to ES VRH, there is another, less studied low T crossover, between VRH and a simple activation dependence (SAD) [33]. For the SAD the temperature behavior of resistivity is described by (1) but with the exponent $p = 1$. Actually, the SAD may occur for different reasons. At high T it could indicate the nearest neighbor hopping (NNH) [23, 34–36], or a band conductivity [6, 37]. At low T, however, the probability of both the NNH and band conductivity becomes negligibly small. Thus, the SAD at low T is usually associated with a hard gap (HG) in the DOS [38], that is, in a certain energy range $g|E| \approx 0$. One of the reason of the HG in doped semiconductors could be the Coulomb interaction [39, 40]. The manifestation of these mechanisms depends not only on the concentration of the main impurities N_d, but also on the degree of compensation of the semiconductor, K.

Traditional Mott, ES, and NNH mechanisms are based on hops to the empty impurity centers. Therefore, the availability of sufficient number of empty donor cites is important for such kind of hops in n-type semiconductor. At low temperatures, this can only be achieved by compensation of semiconductor. Arisen due to compensation charged donors and acceptors create dispersion of the donor energy levels due to their chaotic potential. This dispersion exceeds significantly the exponentially small splitting of levels of neighbor donors caused by the overlap of the wave functions. The characteristic feature of noncompensated semiconductor ($K \ll 1$) is the rapid decrease of the empty (ionized) donors with decreasing temperature. In weakly compensated semiconductors, in a limited range of concentrations (close to the MIT), in addition to the band and hopping conductivity another activation mechanism develops in the temperature dependence of conductivity, ϵ_2 conductivity. This mechanism exhibits in the intermediate between band and hopping conductivity temperature interval [41–43]. It is believed that the ϵ_2 conductivity involves migration of electrons on the single occupied neutral donors (D^- states). They have large radius and, consequently, at the intermediate impurity concentrations are strongly overlapped. The result is a wide band of D^- states. This band is an analogue of the upper Hubbard band (UHB), formed in a disordered systems [6]. The decrease in donor impurity concentration leads to a strong narrowing of a D^- band. On the other hand, in the absence of compensation, when ϵ_3 conductivity is zero, there are most favorable conditions for ϵ_2 conductivity; that is, the concentration of neutral donors is the highest. The increase of the compensation improves significantly conditions for the ϵ_3 conductivity and worsens the ϵ_2 conductivity.

Electron hopping (ϵ_3 conductivity) may occur not only on free localized but also on occupied sites via the spin dependent transport [44]. In fact, for doped semiconductors, the spin degree of freedom could play a significant role in the electron hops. If, for example, the width of the distribution function of the energies of the localized sites overcomes the

Coulomb repulsion between electrons, double occupancy of the site becomes possible, as was first argued by Kurobe and Kamimura [44]. In this case, two types of hops contribute to the transport. The first occurs between singly occupied (SO) and unoccupied (UO) sites, while the second type of hops involves doubly occupied sites (DO) with opposite electron spins. As a result, the spin dependent charge transport could occur in this case. The UO site is considered as a singly ionized site with the elementary charge $+1e$. Consequently, SO site has charge $0e$, and DO site has charge $-1e$. Developing of a quantitative theory of the ϵ_2 conductivity faced with very great difficulties. The main difficulty is that in this concentration range the overlap of the wave functions play a role comparable to the Coulomb interaction of electrons with impurities and with each other. In addition, disorder in the distribution of impurities significantly complicates the analysis of experimental data. Therefore, many problems related to the interpretation of the experimental data for doped semiconductors, in which ϵ_2 conductivity is observed, are still unclear. In this regard, for doped semiconductors with a low degree of compensation, in which ϵ_2 conductivity is manifested, the study of the mechanisms of low temperature conductivity and crossover between ϵ_2 and hopping conductivity is a topical problem.

Therefore, the correct interpretation of the experimental $\rho(T)$ data measured in a wide T range can be significantly hampered, because, in order to compare the experimental values of the parameters with the calculated ones, it is important to identify and properly describe the transport mechanisms in different temperature intervals.

In this work we performed a thorough investigation of the low temperature ($2\,K < T < 90\,K$) conductivity of n-type noncompensated silicon close to the MIT taking into account possible VRH, SAD, and spin dependent mechanisms. We show that above 30 K the conductivity is of the activation type and is carried out in the UHB, while in the T range 5–25 K the Mott-type VRH dominates and is accompanied by the spin dependent charge transport. Below 5 K the crossover from the VRH to SAD occurs. We demonstrate that the reason for the SAD in this T range is the HG in the DOS. We developed a model of this crossover based on the percolation task, using the expression for DOS, which takes into account the evolution of the DOS from the HG at $T < 5\,K$ to the Mott-type at $T > 5\,K$. This approach allowed us to fit the experimental $\rho(T)$ dependence with high accuracy.

2. Samples and Experimental Details

Single crystalline n-type Si (100) grown by Czochralski method and doped with Sb was used in this work. Samples of rectangular shape with a width of 1 mm and a thickness of 0.5 mm were covered with 6 indium contacts as electric probes using ultrasonic soldering. Two contacts were for current supply, 2 were for Hall measurements, and, finally, last 2 contacts were for voltage measurements. All contacts were ohmic in the whole studied temperature range which was proved by the linear current-voltage characteristics. A dc current of $10\,\mu A$ generated by multimeter Keithley 6430 was

used to bias the sample during the resistivity measurements and to measure the voltage drop down to $5\,\mu V$. For low resistivity samples we used the two-channel nanovoltmeter Keithley 2182A. Samples were inserted into the cryogen free measuring system (Cryogenic Ltd., London) with the superconducting magnet. The system allowed performing measurements in the T range between 2 and 300 K in magnetic fields up to $H = 80\,kOe$. Lakeshore controller allowed 0.1 K/min sweeping rate of temperature during the ρ versus T measurements and stabilizing temperature with the accuracy of $\pm 0.005\,K$ during the sweep of the magnetic field or current-voltage characteristics acquisition. Semiconducting GaAs thermometer was calibrated with an accuracy better than 0.1%. On the basis of measurements of the T dependence of the Hall effect the Sb concentration was estimated as $N_d = 1 \times 10^{18}\,cm^{-3}$, which is 3 times less than the critical Mott concentration for Sb in Si [45, 46]. Therefore, our samples are on the insulating side of the MIT. Actually, a series of samples cut from different Si wafers belonging to the same technological set of fabrication were measured. All the data are in nice agreement with each other. Here we present typical results obtained on the investigated samples.

2

3. Results

In Figure 1 we show the resistivity versus temperature measured in the range 2–300 K at zero magnetic field and at the maximum applied field of 80 kOe. The strong change in ρ (4 orders of magnitude) is evident. The $\rho(T)$ dependence at $H = 0$ is linear in the Arrhenius coordinates in the temperature range 28–300 K, as is clearly seen from the inset to Figure 1. Actually, in this temperature interval there are two significantly different activation energies: $\epsilon_1 \approx 10.35\,meV$ for the T range 110–300 K and $\epsilon_2 \approx 1.73\,meV$ for 28–90 K. Resistivity in the first T range is increased by two times, while in the second interval it is increased by only 1.2 times.

Below 20 K at $H = 0$ the SAD is changed to the Mott-type VRH. In Figure 2(a) we show the $\ln\rho(T^{-1/4})$ data for the temperature interval 5–20 K (red color). The obtained in these coordinates linear dependence unambiguously proves the Mott-type VRH. At $T < 5\,K$ the Mott-type VRH is no longer valid and crossover to the SAD with the exponent $p = 1$ and activation energy $\epsilon_4 \approx 1.48\,meV$ occurs (blue color).

Data at $H = 80\,kOe$ below 20 K reveal similar features as for zero field. However, only on the basis of the exponent p in (1) we cannot successfully fit experimental data in the T range 5–20 K. As it follows from Figure 2(b), red symbols, exponent $p = 1/4$ is not suitable to describe the experimental dependence. Other reasonable exponents in (1) also do not give satisfactory agreement with the experiment. Nevertheless, at lower T we can identify interval, where the exponent $p = 1$ is valid, see blue color in Figure 2(b). It turns out that low T SAD still exists even at high magnetic field.

For a more accurate identification of the observed low T SAD in Figure 3 by symbols we plot $\ln\rho$ versus T^{-p} dependence at zero field for two different p values, 1/2 (blue color, corresponds to SE VRH) and 1 (red color, corresponds
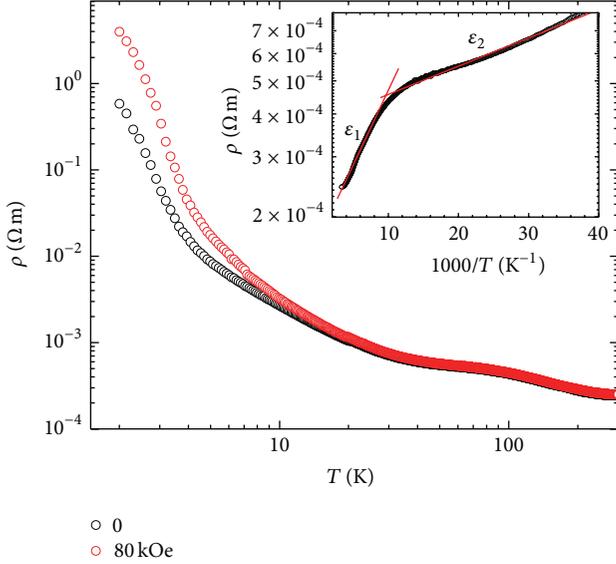
FIGURE 1: Temperature dependence of the resistivity at $H = 0$ (black circles) and $H = 80$ kOe (red circles) in the range 2–300 K. Inset: resistivity versus T^{-1} (symbols). Experimental data are explained by two activation energies, $\epsilon_1 \approx 10.35$ meV for 110–300 K and $\epsilon_2 \approx 1.73$ meV for 28–90 K.

to SAD). Solid lines in Figure 3 correspond to the result of the best linear fit. It follows from Figure 3 that exponent $p = 1/2$ gives worse agreement with the experiment. The same analysis for data measured in the presence of the magnetic field leads to similar result, namely, presence of SAD below $T = 4$ K.

4. Discussion

4.1. Qualitative Analysis. The obtained experimental data revealed the following. In the T interval 110–300 K the conventional band edge activation caused by the transition from the Fermi level located in the tail of the lower Hubbard band (LHB) to the conduction band of silicon (the ϵ_1 conductivity [6]) takes place.

Another simple activation mechanism is manifested in the temperature dependence of the resistivity in the interval 28–90 K (ϵ_2 conductivity). It is believed that the ϵ_2 conductivity is associated with the activation motion of electrons along singly occupied neutral donors and corresponds to the states in the upper Hubbard band (UHB) [5, 6, 20, 37]. In this temperature interval the characteristic value of the thermal energy $k_B T$ is greater than the activation energy ϵ_2 and all states are delocalized. Moreover, only slight increase in the resistivity as the temperature decreases or magnetic field increases indicates the extended UHB.

In the T range 5–20 K the Mott-type hopping ϵ_3 conductivity is observed in the absence of the magnetic field. Finally, in the temperature interval 2–4 K again the SAD with the activation energy $\epsilon_4 \approx 1.48$ meV is realized. At first glance, this is a reentrance of the previously observed within the temperature interval 28–90 K SAD with the activation energy

$\epsilon_2 \approx 1.73$ meV. On the other hand, for the range 2–4 K the activation energy ϵ_4 is greater than the energy of thermal fluctuations, $\epsilon_4 \approx (3–7)k_B T$. It means that all states are localized; that is, the charge transport is hopping-like, but the mechanism of hops is different from usual VRH.

The reentrance of the SAD after VRH is well known for some dilute magnetic [38, 47, 48] and classical doped semiconductors, like Si:B [33] and Si:As [49] with doping concentration less than N_c, and for amorphous compounds like In/InO$_x$ [50] or amorphous silicon after implantation of Au or Si ions [51]. For all these materials evidences of ϵ_2 conductivity before VRH were never reported. Typically, as T decreases first one observes the NNH, which is characterized by the exponent $p = 1$, then the VRH followed by SAD, again with the exponent $p = 1$. Moreover, for dilute magnetic semiconductors and for Si:B strong magnetic field removes the reentrance effect. But for In/InO$_x$ the reentrance effect is insensitive to the magnetic field [50]. It is worth mentioning that for the electronic Si:As semiconductor the influence of the magnetic field on the reentrance effect was not studied. In our system, the reentrance effect in the presence of the magnetic field still does exist, see Figure 2(b). Moreover, the peculiar feature of the appearance of the SAD reentrance in our case is that not only the VRH, but also the ϵ_2 conductivity (not NNH) preceded it.

Thus, the performed brief qualitative analysis of the data disclosed that, in the range 28–90 K, the influence of both the temperature and magnetic field on the resistivity is very low. This indicates that the electron transport in this temperature range has apparently a band character, is realized in the relatively wide UHB and states are delocalized. In the range 5–20 K the electron transport is transformed to the hopping ϵ_3 conductivity. With further T decrease, below 4 K, the Mott-type VRH is transformed into more complicated hopping mechanism which formally corresponds to the SAD, but now states are localized.

Actually, the SAD at low T indicates the formation of the HG in the DOS [38]. The energy ϵ_4 characterizes the width of the HG, where the DOS is equal or close to zero. The magnetic field does not suppress the SAD. The reason of the HG appearance is hidden. In order to understand better the nature of the reentrance effect and the origin of the HG, we need to perform the quantitative analysis of the data.

4.2. Quantitative Analysis

4.2.1. Spin Dependent Hopping. For the T range 5–20 K the resistivity is described according to the Mott law, (1) [3, 6], in which $T_h = T_M$ and $p = 1/4$. Here $T_M = \beta_M [g_M a_M^3 k_B]^{-1}$ is the Mott parameter, $\beta_M = 21.2 \pm 1.2$ is the numerical factor, $g_M = $ const is DOS at the Fermi level, a_M is the localization length of the states around the Fermi level. We calculated the g_M and a_M values analyzing the experimental data $\rho(T)$ at
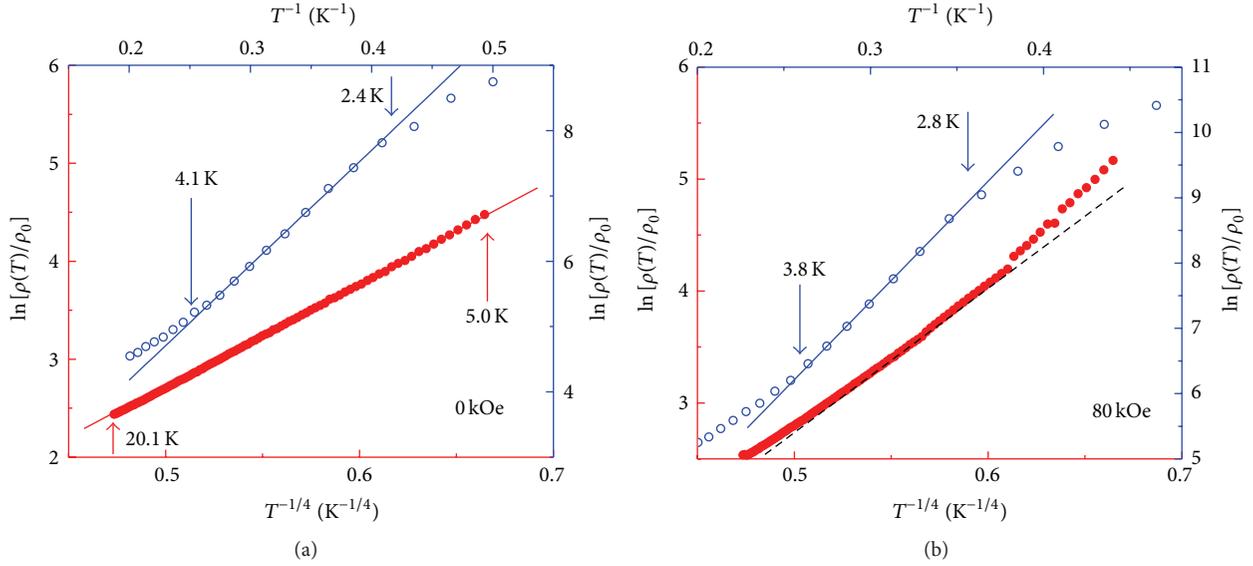
FIGURE 2: (a) $\ln \rho$ versus $T^{-1/4}$ (red symbols), left and bottom red axis. $\ln \rho$ versus T^{-1} (blue symbols), right and upper blue axis. Solid lines are the result of the best linear fit in these coordinates. Data are for $H = 0$. (b) $\ln \rho$ versus $T^{-1/4}$ (red symbols), left and bottom red axis. $\ln \rho$ versus T^{-1} (blue symbols), right and upper blue axis. Solid blue line is the result of the best linear fit in these coordinates. Dashed black line is tangent to the experimental data. Data are for $H = 80$ kOe.
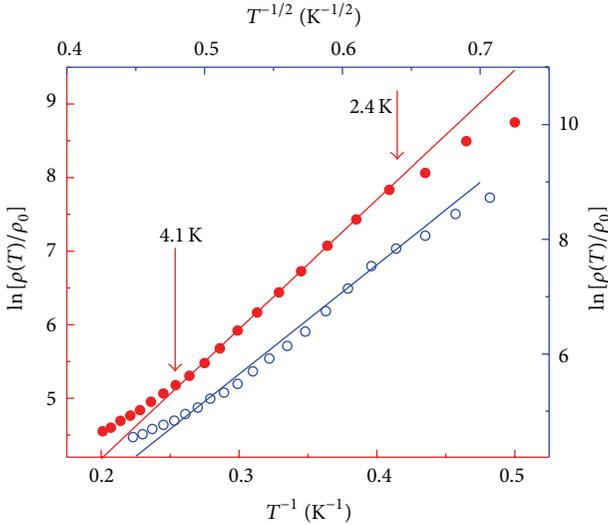

FIGURE 3: $\ln \rho$ versus T^{-1} (red symbols), left and bottom red axis. $\ln \rho$ versus $T^{-1/2}$ (blue symbols), right and upper blue axis. Solid lines are the result of the best linear fit in these coordinates. Data are for $H = 0$.

zero magnetic field in the Mott coordinates ($\rho - T^{-1/4}$) and applying the evaluation expressions [3, 6, 52, 53]

$$g_M = \frac{N_d}{2k_B \left(T_M T_{vM}^3\right)^{1/4}},$$
$$a_M = \frac{\beta_M^{1/3}}{\left[k_B T_M g_M\right]^{1/3}}, \tag{2}$$

TABLE 1: Parameters of the Mott-type VRH obtained within two different approaches.

Parameter	$\rho(T)$ data	MR data
a_M, nm	6.6	6.0–8.5
g_M, eV$^{-1} \times$ cm^{-3}	5.408×10^{19}	4.7×10^{19}

where T_{vM} is the temperature of the onset of the Mott-type VRH. Equation (2) gives approximate values of g_M and a_M. Note that on the basis of (1) and (2) the obtained g_M and a_M values must be temperature independent. On the other hand, the MR data allow checking whether these quantities are really T independent. Indeed, within the standard approach of the Mott-type VRH the positive MR which is usually related to the contraction of the wave function of the localized states in magnetic field is expressed as [6]

$$\ln \frac{\rho(H)}{\rho(0)} = t_3 \frac{a_M^4}{l_H^4} \left(\frac{T_M}{T}\right)^{3/4} \sim H^2, \tag{3}$$

where numerical factor $t_3 = 5/2016$, $l_H = \sqrt{\hbar/e\mu_0 H}$ is the magnetic length, and $\rho(0)$ is the zero field resistivity.

On the basis of (3), knowing T_M, H, and MR, we calculated the a_M values at different T. Moreover, knowing already a_M, the value of g_M from results of the MR measurements can be calculated using the expression for the Mott parameter T_M.

The results of calculations of hopping parameters according to the $\rho(T)$ dependence and MR data at different T are summarized in Table 1. The Mott parameter was evaluated from (1) as $T_M = 1.524 \times 10^4$ K. The temperature T_{vM} was obtained from the $\rho(T)$ data as $T_{vM} \approx 20$ K [54].
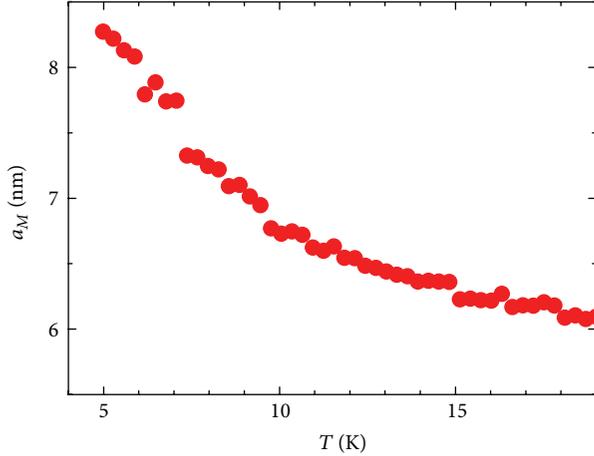
FIGURE 4: Temperature dependence of the localization length a_M. Data are for $H = 80$ kOe.
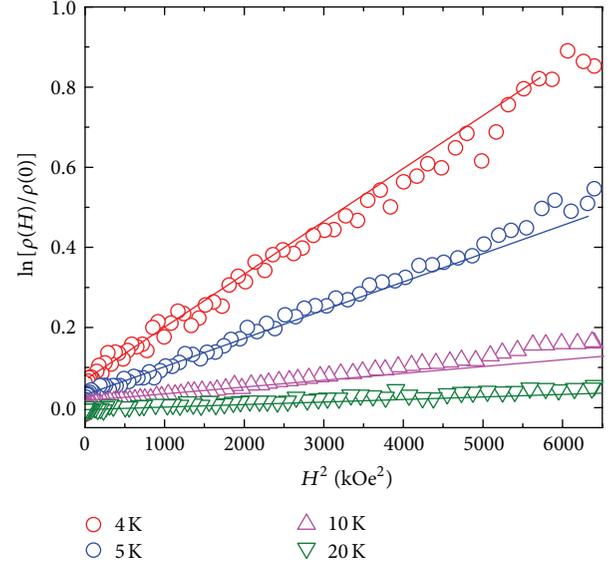

FIGURE 5: $\ln(\rho(H)/\rho(0))$ versus H^2 at different temperatures (symbols). Lines correspond to the results of the best linear fit in these coordinates.
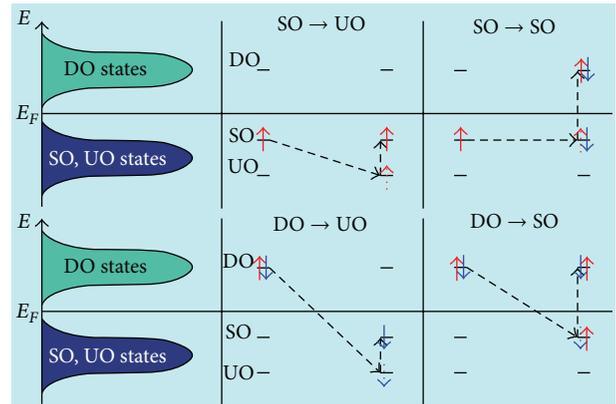

FIGURE 6: Possible electron hops considered for low temperature conductivity. For more details, see the text.

It follows from Table 1 that the obtained within two different approaches a_M and g_M values are in good agreement with each other.

The surprising result, which we obtained, analyzing the a_M values from the MR measurements, is their T dependence. This result for $H = 80$ kOe is presented in Figure 4, from which it follows that the $a_M(T)$ function is not constant. In particular, for the range 5–20 K the a_M values decrease from 8.3 to 6.0 nm. This means that the standard model of positive MR, which takes into account only the contraction of the electronic wave function in magnetic field and leads to the temperature independent localization length, cannot explain the obtained $a_M(T)$ result.

In Figure 5 we show the dependencies of $\ln(\rho(H)/\rho(0))$ versus H^2 in the temperature range 4–20 K together with the results of the best fit procedure according to (3). It is seen that the $\ln(\rho(H)/\rho(0)) \sim H^2$ law in the considered temperature range is valid only at $H < (50$–$60)$ kOe. From the results presented in Figures 2(b), 4 and 5 it follows that the transport mechanism at low T becomes more complicated than conventional Mott-type VRH. To clarify the hopping mechanism, we examine other possible types of hops, to the occupied localized sites, which are accompanied by a spin flip [44].

The MR for a system of sites occupied by more than one electron was considered in detail some time ago by Kurobe and Kamimura [44], Matveev et al. [55], Meir [56], and Demishev and Pronin [57]. In particular, if the Coulomb repulsion between two electrons is smaller than the width of the Hubbard bands, 2 types of hops, on unoccupied (SO → UO, DO → UO) and occupied (SO → SO, DO → SO) sites are relevant. All these possibilities are shown in Figure 6, where we schematically draw the energy diagrams for each type of hops.

In general case, spin independent hops to unoccupied sites could be characterized by the localization length a_1 and DOS g_1, while spin dependent hops to occupied sites could be described, in turn, by a_2 and g_2. The quantity g_1 is assigned to the DOS in the LHB, and g_2 corresponds to the DOS in

the UHB. The relation between g_1 and g_2 as well as between a_1 and a_2 is still an open question and different assumptions were put forward to simplify the task. Typically, it is assumed that the localization length for the DO state is more than for the SO, $a_2 > a_1$ [44]. In [56] the possibility of spin dependent transport was discussed considering inequality between two densities of states and two localization lengths. From a practical point of view, it seems problematic to separate these quantities in the framework of such general approach. It is necessary to introduce additional assumptions associated with the density of states or the localization length.

In [55] the spin polarized mechanism of MR was investigated in terms of the approach proposed by Kurobe and Kamimura [44]. It was supposed that both the states, UO and SO, are characterized by the same localization length, $a_1 = a_2 = a$, while densities of states differ from each other, $g_1 \neq g_2$.

We failed in the attempts to fit the experimental data of Figure 2(b) applying theoretical approaches of Refs. [55, 56]. We believe this is due to the fact that applied theoretical approaches do not take into account all complexity of the transport mechanisms. Further we investigate this problem in detail within the approach proposed by Demishev et al. [57, 58]. Authors [57], following Kurobe and Kamimura [44], considered only intrasite correlations and neglect the long range Coulomb repulsion. On the basis of [57] it is possible to determine which type of conductivity under the external magnetic field dominates: spin dependent or spin independent. In particular, the modified expression for the MR, which takes into account both types of hops, was deduced [58]:

$$\ln \frac{\rho(H)}{\rho(0)} = \left(\frac{T_M}{T}\right)^{1/4} \frac{1}{4} A_{\text{eff}}(T) \left(\frac{\mu_0 \mu_B H}{k_B T}\right)^2, \quad (4)$$

where

$$A_{\text{eff}}(T) = A + 4b \left(\frac{T}{T_M}\right)^{3/2}. \quad (5)$$

In (5) parameters $A = (g_2 a_2^3 - g_1 a_1^3)/(g_2 a_2^3 + g_1 a_1^3)$ and $b = t_3 a_2^4 (e^2 k_B^2 T_M^2 / \hbar^2 \mu_B^2)$. According to Demishev et al. [58], parameter A depends on the probability of hops, which involve both D^0 and D^- states, and is determined by the degree of polarization of the spin part of the wave function of these states in the magnetic field. Parameter b is determined by the contribution of the mechanism of the wave function contraction to the MR that acts on both types of hops.

Therefore, on the basis of the temperature dependence $A_{\text{eff}}(T)$ it is possible to conclude which type of contribution determines the MR in the hopping region. If the spin dependent mechanism dominates, then $A_{\text{eff}}(T) = \text{const}$. Otherwise, $A_{\text{eff}}(T)$ tends to 0 at $T \to 0$ according to the law $T^{3/2}$. When both types of contributions are comparable, the dependence of $A_{\text{eff}}(T)$ is expected to be more complicated, it does not tend to 0 at $T \to 0$ [57, 58].

In Figure 7 we plot the $A_{\text{eff}}(T)$ dependence obtained from the experiment applying (4). Data are for $H = 80$ kOe. As can be seen, the $A_{\text{eff}}(T)$ dependence has two distinct regions. In one of them, in the T range 5–11 K, the A_{eff} value is temperature independent and the results of the fitting procedure give $A = 0.47 \pm 0.03$, $b = 0$ (blue line in Figure 7). Therefore, in this T range the spin dependent hopping prevails. In addition, the relation between DOS for two different types of hops can be estimated via the quantity $k_g = g_2 a_2^3 / g_1 a_1^3$. In this case $k_g \approx 2.8$.

In the T range 11–20 K the linear approximation $A_{\text{eff}}(T) \sim T^{3/2}$ explains well the experimental data (red line in Figure 7), but A_{eff} does not tend to 0 at $T \to 0$. Consequently, the obtained result proves the absence of the dominant role of the spin independent hops in this temperature interval. From the fitting procedure we obtained coefficients $A = 0.29$ and $b = 0.96 \times 10^4$. That gives $a_2 = 5.5$ nm and $a_1 \approx a_2/4 = 1.38$ nm. The parameter k_g in this case depends on T. The obtained overall $k_g(T)$ dependence is shown in the inset to Figure 7.
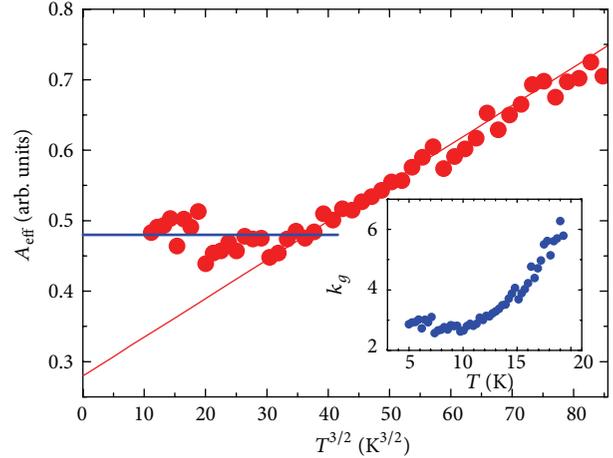

FIGURE 7: Evaluated temperature dependence $A_{\text{eff}}(T)$ at $H = 80$ kOe (symbols). Lines are plotted according to (5). Inset: the temperature dependence of the calculated coefficient k_g.

From k_g values we may estimate the g_1/g_2 relation, which is equal to 21.3 for T range 5–10 K and to 10.7 at $T = 20$ K.

4.2.2. Gap in the DOS. Thus, the performed estimations and calculations showed that, in the temperature range 5–20 K, on the whole, the Mott-type VRH is realized. Nevertheless, we obtained that two types of hops, traditional hops on UO sites and spin dependent hops on SO sites, have to be taken into account. Therefore, one needs to consider two localization lengths and two DOS. On the other hand, previously introduced g_1 and g_2 values are essentially model parameters that do not give information about the influence of the DOS on the mechanism of hopping conductivity. It should also be noted that neither approach [55] nor work [57] gives any information about the gap between two Hubbard bands.

Generally speaking, the origin of the gap could be twofold. First, it could be due to the CG; second, the HG between lower and upper Hubbard bands could be the reason. The soft CG at the energy minimum does not have a characteristic shelf, $g(E) \sim |E - E_F|^2$, while the true gap has the shelf of the width Δ. Moreover, the presence of the soft CG leads to the exponent $p = 1/2$, which we did not observe.

Below we propose the model expression for the DOS and evaluate the influence of the shape and parameters of the proposed model DOS on the T dependence of the hopping resistivity, which, in turn, is characterized by the critical values of the exponent $\xi(T) = \ln[\rho(T)/\rho_0]$ [21]. The relation between the critical exponent $\xi(T)$ and the exponent p is $\xi(T) \sim (T_h/T)^p$. Estimations are performed within the model of the low temperature crossover VRH-SAD.

To model this crossover let us consider the problem of the charge flow in the lattice of impurity atoms. In the theory of hopping conductivity, problems of charge flow in the system of random nodes, chaotically distributed in space, play the most important role. In this case the average number of nodes in a unit volume is supposed to be given and

equal to the concentration of the impurities N_d. The average distance between nodes is $r_d = (3/4\pi N_d)^{1/3}$. For such a lattice, the percolation radius r_c is found from the condition of the connectivity of two and more nodes which form an infinite cluster [6], so that the value of r_c depends only on the nodes concentration N_d. Typically, the dimensionless threshold value B_c is used, having a meaning of the average number of bonds per node. In the 3D case [6]

$$B_c = \left(\frac{4\pi}{3}\right) r_c^3 N_d. \qquad (6)$$

For random lattice the B_c value is typically determined numerically and varied in the range 2.65–2.76 [6]. Consequently, the percolation radius is given by $r_c = (0.865 \pm 0.015) N_d^{-1/3}$. In this case r_c is always larger than r_d. In particular, in our case $r_c = 8.64$ nm $> r_d = 6.2$ nm. In other words, the symmetry of the lattice is irrelevant and only the number of sites inside radius r_c determines the transport mechanism.

On the basis of the aforementioned estimations, we then developed a model of the VRH-SAD crossover; this model is based on a simplified procedure for solving the percolation problem using the empiric expression for the DOS valid for both types of the temperature dependent hopping. We start from the following expression for the dimensionless concentration of sites:

$$N(\xi) = 2 \int_0^{E_{max}} r_{max}^3 g(E) \, dE, \qquad (7)$$

which satisfies the condition of connectivity for the exponent of the hopping resistivity less than a certain value ξ_{min} [6, 13]. Here, E_{max} and r_{max} are maximal values of the energy and intersite spacing, respectively, which still allow the connectivity. The dimensionless concentration $N(\xi)$ in (7) is determined as a product of the concentration of sites with the energy $E < E_{max}$ and the volume of these sites. This procedure for the temperature dependent DOS is not completely rigorous and the connectivity condition should be considered for each energy value separately, which leads to the complicated integral equation [13]. Here we will follow the procedure described in [21], which simplifies significantly the calculations.

Values of r_{max} and E_{max} are specified in the percolation theory by the relations [6] (see also Equation (4.30) in [59])

$$r_{max} = \frac{a_2 \xi}{2}, \qquad (8)$$
$$E_{max} = k_B T \xi.$$

Substituting (8) into (7) and equating $N(\xi)$ to $2B_c$, we get the following expression:

$$2B_c = \left(\frac{a_2 \xi}{2}\right)^3 \int_0^{k_B T \xi} g(E) \, dE, \qquad (9)$$

which allows calculating the T dependence of ξ and compare it with the experimental data $\rho(T)$. The above procedure was
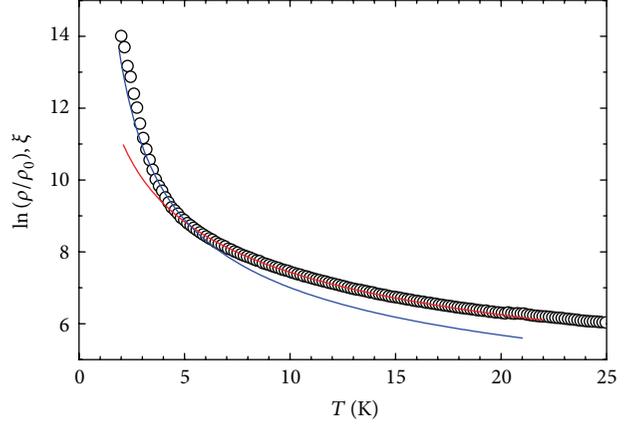

FIGURE 8: Experimental (symbols) $\ln[\rho(T)/\rho_0]$ and calculated (lines) according to (10) $\xi(T)$ dependencies. Red and blue lines correspond to $n = 0$ and 15, respectively.

carried out using three different types of expressions for the DOS.

First, we used the interpolation expression proposed in [22, 23]. Thus, the change of the DOS from constant value for the VRH Mott-type to the DOS $g(E) \sim |E - E_F|^n$, where for the SAD $n > 2$, was taken into account. In this case the DOS models, presumably, only the CG-*like*, but with steeper dependence on the energy. According to [22], the crossover at different exponent values of $p = (n + 1)/(n + 4)$ could be described applying the following expression for the DOS:

$$g(E, T) = g_0 \frac{\left[(E - E_F)/E_{sg}\right]^n}{1 + \left[(E - E_F)/E_{sg}\right]^n}. \qquad (10)$$

Parameter E_{sg} depends on the exponent n and, when it is fixed, is constant. Parameter g_0 is a constant related to g_M. For the case $n = 2$, (10) coincides with the expression used in [14] for the description of the crossover from the Mott to ES VRH.

Substituting (10) into (9) and using the previously obtained values, a_2 and $E_{sg} = \epsilon_4$, we calculated the dependencies $\xi(T)$ for the fixed values of the exponent n in (10), which were compared with the experimental data $\ln[\rho(T)/\rho_0]$. We obtained that theoretical results coincide with the experimental data only varying values of the exponent n with temperature [60]. For example, in the interval 5–25 K the agreement is observed only for $n = 0$ (the Mott-type VRH), while for 2–5 K to obtain the agreement between theory and experiment much greater value of n, $n > 6$, is required, Figure 8. Calculations of the $p(T)$ dependencies for different n values using the relation $p = -\partial \log \xi(T)/\partial \log T = -[T/\xi(T)][\partial \xi(T)/\partial T]$ [21] and evaluated the $\xi(T)$ dependence showed that, to achieve the value of the exponent p, close to unity, it is necessary to significantly increase n, that is, the variable n needs to tend to infinity, Figure 9. At $n = 0$ expressions for the crossover give the exact value $p = 1/4$. Thus, (10) for the DOS in this case has limited application because, firstly, it requires a change of the exponent n with
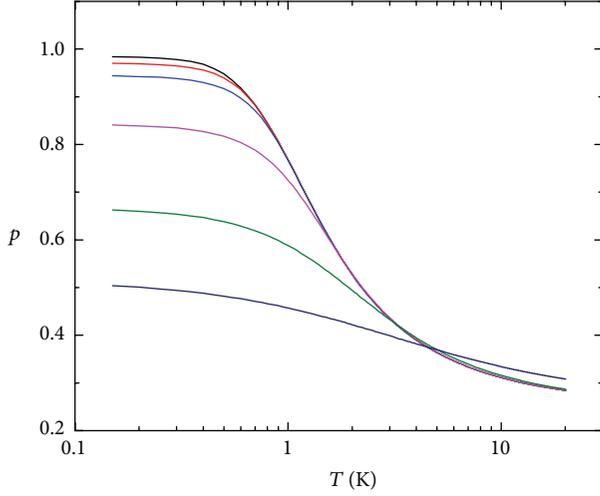
FIGURE 9: Temperature dependencies of the exponent p for different n values. From top to down, $n = 200, 100, 50, 15, 5$, and 2, respectively.

T and, secondly, the value of n, which provides the exponent $p \to 1$, tends to infinity.

In the second attempt, we take into account the gap smearing with T increase [61],

$$g(E, T) = g_0 \left[\gamma(T) + [1 - \gamma(T)] \frac{|E - E_F|^n}{[\Delta(T)/2]^n + |E - E_F|^n} \right]. \quad (11)$$

The parameter γ describes a "residual" DOS at the Fermi level and Δ is the width of the gap.

Substitution of the modified expression (11) to (9) allowed comparing the value of the critical exponent ξ with the experimental data and finding the temperature dependencies $\gamma(T)$ and $\Delta(T)$, which adequately describe the experiment. This result is presented in Figure 10 for two n values, $n = 2.5$ and 3.0.

It follows from Figure 10 that γ varies in the range 0.1–1. At $T > 10$ K, $\gamma \to 1$, and the first constant term in (11) dominates. This corresponds to the Mott-type VRH. When $\gamma = 1$ (i.e., at $T > 15$ K), the result becomes insensitive to the Δ values. At low temperatures $\gamma \ll 1$ and the main contribution is due to the term $|E - E_F|^n$. The parameter Δ, which characterizes the width of the gap, decreases with increasing temperature, which is in contradiction with the result usually reported [61, 62]. Thus, the result of the fitting procedure found that the agreement with the experiment is achieved only taking into account the filling of the gap states between the Hubbard bands and suggested the narrowing of the gap with increasing temperature, during the crossover to the Mott-type DOS. In addition, insensitivity of the model to the value of n at $n > 3$ has been revealed. Therefore, it is obvious that there is a need to modify the formula for the DOS, in order to reflect the tendency both for smearing of the gap and its growth with increasing temperature. These are characteristic features of the HG. Moreover, the integer exponent n should be temperature independent.
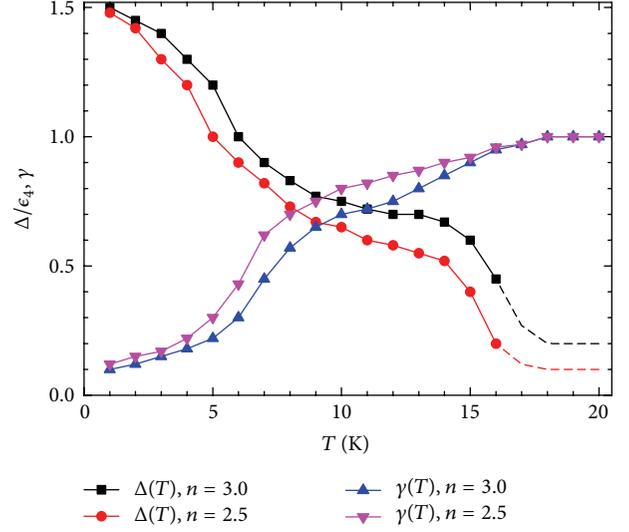

FIGURE 10: $\gamma(T)$ and $\Delta(T)$ dependencies as obtained using (11) for fitting the $\rho(T)$ data. Calculated curves correspond to the range of the exponent $n = 2.5$–3.0. The γ values are in arbitrary units. The Δ values are normalized to ϵ_4.
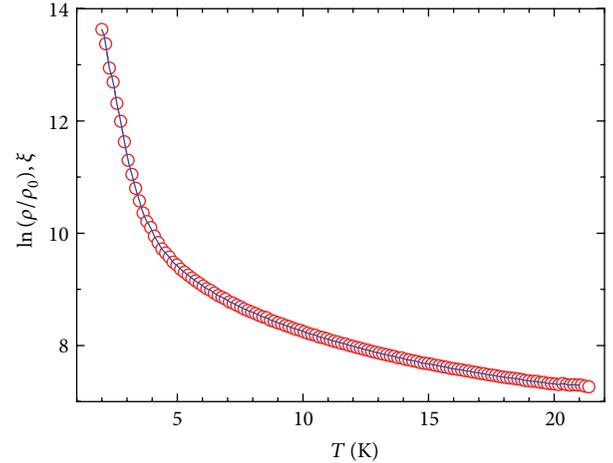

FIGURE 11: Experimental (symbols) $\ln[\rho(T)/\rho_0]$ and calculated (lines) according to (12) $\xi(T)$ dependencies.

Within these assumptions the reasonable approximation for the DOS is of the following empiric type:

$$g(E, T) = g_0 \left[\alpha(T) w^4(E) + \beta(T) w^2(E) + \gamma(T) \right] \\ \times \exp\left(-\left[\frac{w(E)}{\sigma(T)} \right]^4 \right), \quad (12)$$

where $w(E) = (E - E_F)/0.5\epsilon_4$ and α, β, γ, and σ are phenomenological *temperature dependent* coefficients.

The shape of the DOS in this case depends on T according to the α, β, γ and σ versus T dependencies. In particular, the first term corresponds to the HG, the second one is for the soft gap, the parameter γ is responsible for the filling of the HG with T and σ is responsible for the width of the Hubbard band. Indeed, the exponential term serves for smoothing of

the overall DOS and for modelling of the Hubbard bands, in particular, their width. In other words, empirical expression (12) allows reproducing not only the HG, its filling, but also the width of the Hubbard bands. In this work, we assumed the identical widths of the upper and lower Hubbard bands. Widening of the UHB was taken into account by filling the HG. Function (12) reflects the change of the DOS with T, from HG at low T (with the dip between Hubbard bands) to the constant DOS close to the Fermi level at high T. This was enough for the experimental data interpretation. The fitting procedure was as for previous expressions for the DOS; that is, we substitute (12) into (9) and looked for such ξ values which adequately describe the $\rho(T)$ data. The result of the fitting procedure is shown in Figure 11. It follows that we were able to describe experimental data with very high accuracy in the T range 2–20 K. On the basis of the obtained $\xi(T)$ dependence it is possible to evaluate r_{max}, the maximal hopping length which still allows the connectivity. For the range 5–20 K we get $r_{max} = 17.6–22.0$ nm, while for the interval 2–4 K the result is $r_{max} = 27.5–38.5$ nm.

On the basis of the obtained model parameters, it is possible to reproduce the DOS at different temperatures. This result is shown in Figure 12. As it follows, the DOS evolves from HG at 2 K to almost filled states between Hubbard bands at 15 K. At that the widening of the Hubbard bands also occurs (within our approach, UHB and LHB are symmetrical; actually, they may differ in width and height, but this issue requires additional investigation and is outside the objectives of this work). Parameters of the model are changed as follows. The parameter α, which corresponds to the HG width is almost constant and is equal to 1 for the whole T range. The parameter β (characteristic of the soft gap) is almost constant with temperature, $\beta = -0.7$ except the region 15–21 K, where $\beta = -2$. The parameter γ, which is responsible for the HG filling, is changed from 0 at 2 K to 6 at 21 K. Finally, the parameter σ, the characteristic of the width of the Hubbard bands, also increases with temperature, from 1.5 to 2.3.

At the end of this section we summarize that, the conductivity in the T interval 5–20 K is of the hopping-type. On the whole, it obeys the Mott law and is determined by two type of hops: to UO neutral and to SO impurity sites. In the range 5–11 K the contribution of the spin dependent hopping dominates. This is valid also in the range 2–4 K. Simulations of the DOS revealed that in this T range hops are regulated by the HG. The presence of nonsmeared HG between Hubbard bands in the T range 2–4 K together with the spin dependent hops in the UHB provides reentrance of the SAD. *The latter provides a nonlinearity of the current-voltage characteristics at small bias voltage, which leads to negative differential resistance at electrical fields smaller than 1 V/cm [63]. It is unlikely that this effect may be due to the ES VRH, for which the delocalization occurs at significantly higher electrical fields.*

5. Conclusions

In conclusion, we performed the systematic study of the transport mechanisms in n-type noncompensated Si in the
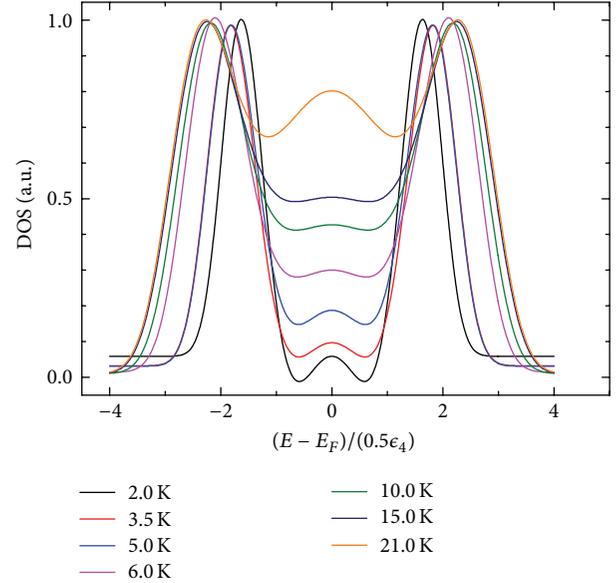

FIGURE 12: DOS at different temperatures as obtained from the experimental data within the proposed model (see (12)).

temperature range 2–300 K. Samples were grown by the Czochralski method, containing donor impurities of Sb with a concentration of 1×10^{18} cm^{-3}, It was found that, depending on the temperature range, it is possible to identify 4 different mechanisms of the electron transport. All of them include the upper and lower Hubbard bands.

In the T range 110–300 K the usual activation to the edge of the conduction band occurs.

At lower T, in the range 2–90 K, the conductivity of silicon is mainly due to the impurities and is caused by the hopping and band electron transport involving two Hubbard bands. In the high T range of this interval (28–90 K) electronic states are delocalized and charge transport occurs via the SO neutral donors, while in the low T range (2–20 K) electronic states are localized and the hopping prevails. The hopping region is characterized by two types of hops, on UO and SO sites, as well as by two modes, the Mott-type and SAD. The Mott regime, in turn, is characterized by two types of hops and two mechanisms of the MR, mainly the spin polarized mechanism in the T range 5–11 K and the mechanism, for which contribution of the spin polarization is approximately equal to the contribution of the wave function contraction (11–20 K). In the T interval 2–4 K the conductivity is governed by the HG and the charge transport is associated mainly with the spin dependent hopping in the UHB. *To improve the identification of the observed Mott-type VRH-SAD crossover and enhance the temperature interval of SAD the energy range of the impurity states as well as the level of the injection of the electrons should be increased [63].*

Simulation of the DOS within the model of crossover between the Mott-type VRH and SAD were carried out for two types of DOS, soft gap and HG. We showed that, the use of the interpolation expression for the CG-like DOS, but with the exponent n greater than 2 and neglecting the gap

smearing, leads to the necessity of noticeable increase of the exponent n to get the exponent $p = 1$ at $T < 4$ K. Simulation of the CG-like DOS taking into account the width of the gap and smearing of the region between Hubbard bands showed that, with increasing T both smearing and decreasing of the gap occurs that does not quite correspond to the T dependence of the soft gap known from literature. Finally, simulation within the HG approach considering smearing, growth of the HG, and widening of the Hubbard bands with increasing T allowed describing with high accuracy the experimental $\rho(T)$ dependence in the low T range 2–20 K. The latter confirms the adequacy of the proposed HG model for interpretation of the conductivity in the range 2–4 K, although more detailed experimental and theoretical studies are required to clarify better the impact of the HG on the low T electron transport. *In particular, direct spectroscopic measurements of the density of states or conductivity measurements for n-type Si with impurities of various energy levels and different compensation degree could be potentially useful for these purposes.*

Competing Interests

The authors declare that there is no conflict of interests regarding the publication of this paper.

Acknowledgments

References

[1] H. V. Löhneysen, "Metal-insulator transition in heavily doped semiconductors," *Current Opinion in Solid State and Materials Science*, vol. 3, no. 1, pp. 5–15, 1998.

[2] V. Dobrosavljevic, N. Trivedi, and J. M. Jr. Valles, *Conductor-Insulator Quantum Phase Transitions*, Oxford University Press, 2012.

[3] N. F. Mott, *Metal-Insulator Transitions*, Taylor & Francis, London, UK, 2nd edition, 1990.

[4] P. P. Edwards and M. J. Sienko, "Universality aspects of the metal-nonmetal transition in condensed media," *Physical Review B*, vol. 17, no. 6, pp. 2575–2581, 1978.

[5] H. Fritzche, in *The Metal Non-Metal Transition in Disordered Systems*, L. F. Friedman and D. P. Tunstall, Eds., p. 130, University of St. Andrews, St. Andrews, UK, 1979.

[6] B. I. Shklovskii and A. L. Efros, *Electronic Properties of Doped Semiconductors*, Springer, Berlin, Germany, 1984.

[7] A. L. Efros and B. I. Shklovskii, "Coulomb gap and low temperature conductivity of disordered systems," *Journal of Physics C: Solid State Physics*, vol. 8, no. 4, pp. L49–L51, 1975.

[8] A. L. Efros, "Coulomb gap in disordered systems," *Journal of Physics C*, vol. 9, no. 11, pp. 2021–2030, 1976.

[9] J. R. Friedman, Y. Zhang, P. Dai, and M. P. Sarachik, "Magnetic-field-induced crossover from Mott variable-range hopping to weakly insulating behavior," *Physical Review B*, vol. 53, no. 15, pp. 9528–9531, 1996.

[10] J. Zhang, W. Cui, M. Juda et al., "Hopping conduction in partially compensated doped silicon," *Physical Review B*, vol. 48, no. 4, pp. 2312–2319, 1993.

[11] A. Fujimoto, H. Kobori, T. Ohyama et al., "Crossover from positive to negative magnetoresistance by the rise of electron temperature for Si:Sb in the variable-range hopping regime," *Physica B: Condensed Matter*, vol. 324, no. 1–4, pp. 1–8, 2002.

[12] A. Aharony, Y. Zhang, and M. P. Sarachik, "Universal crossover in variable range hopping with Coulomb interactions," *Physical Review Letters*, vol. 68, no. 26, pp. 3900–3903, 1992.

[13] Y. Meir, "Universal crossover between Efros-Shklovskii and mott variable-range-hopping regimes," *Physical Review Letters*, vol. 77, no. 26, pp. 5265–5267, 1996.

[14] R. Rosenbaum, N. V. Lien, M. R. Graham, and M. Witcomb, "A useful Mott-Efros-Shklovskii resistivity crossover formulation for three-dimensional films," *Journal of Physics Condensed Matter*, vol. 9, no. 29, pp. 6247–6256, 1997.

[15] L. R. Wienkes, C. Blackwell, and J. Kakalios, "Electronic transport in doped mixed-phase hydrogenated amorphous/nanocrystalline silicon thin films," *Applied Physics Letters*, vol. 100, no. 7, Article ID 072105, 2012.

[16] B. Skinner, T. Chen, and B. I. Shklovskii, "Theory of hopping conduction in arrays of doped semiconductor nanocrystals," *Physical Review B—Condensed Matter and Materials Physics*, vol. 85, no. 20, Article ID 205316, 2012.

[17] S. Nakatsuji, V. Dobrosavljević, D. Tanasković, M. Minakata, H. Fukazawa, and Y. Maeno, "Mechanism of hopping transport in disordered mott insulators," *Physical Review Letters*, vol. 93, no. 14, Article ID 146401, 2004.

[18] M. Salvato, M. Lucci, I. Ottaviani et al., "Transport mechanism in granular Ni deposited on carbon nanotubes fibers," *Physical Review B*, vol. 86, no. 11, Article ID 115117, 2012.

[19] F. A. Zwanenburg, A. S. Dzurak, A. Morello et al., "Silicon quantum electronics," *Reviews of Modern Physics*, vol. 85, no. 3, pp. 961–1019, 2013.

[20] E. Prati, K. Kumagai, M. Hori, and T. Shinada, "Band transport across a chain of dopant sites in silicon over micron distances and high temperatures," *Scientific Reports*, vol. 6, Article ID 19704, 2016.

[21] N. V. Agrinskaya and V. I. Kozub, "Universal description of crossover between the Mott regime and the Coloumb-gap regime in hopping conductivity: application to compensated CdTe," *Journal of Experimental and Theoretical Physics*, vol. 89, no. 6, pp. 1125–1129, 1999.

[22] N. V. Lien and R. Rosenbaum, "General crossovers from two-dimensional Mott $T^{-1/3}$ to soft-gap $T^{-\gamma}$ variable-range hopping," *Physical Review B—Condensed Matter and Materials Physics*, vol. 56, no. 23, pp. 14960–14963, 1997.

[23] N. Van Lien and R. Rosenbaum, "General resistance crossover expressions for three-dimensional variable-range hopping," *Journal of Physics Condensed Matter*, vol. 10, no. 27, pp. 6083–6090, 1998.

[24] P. A. Lee and T. V. Ramakrishnan, "Disordered electronic systems," *Reviews of Modern Physics*, vol. 57, no. 2, pp. 287–337, 1985.

[25] A. Aharoni and D. Stauffer, *Introduction to Percolation Theory*, Taylor & Francis, London, UK, 2nd edition, 1994.

[26] B. I. Shklovskii and A. L. Efros, "Impurity band and conductivity of compensated semiconductors," *Soviet Physics—Journal of Experimental and Theoretical Physics*, vol. 33, no. 2, pp. 468–474, 1971.

[27] V. Ambegaokar, B. I. Halperin, and J. S. Langer, "Hopping conductivity in disordered systems," *Physical Review B*, vol. 4, no. 8, pp. 2612–2620, 1971.

[28] I. S. Beloborodov, A. V. Lopatin, V. M. Vinokur, and K. B. Efetov, "Granular electronic systems," *Reviews of Modern Physics*, vol. 79, no. 2, pp. 469–518, 2007.

[29] E. Dagotto, *Nanoscale Phase Separation and Colossal Magnetoresistance*, Springer, Berlin, Germany, 2002.

[30] D. Shahar, D. C. Tsui, M. Shayegan, E. Shimshoni, and S. L. Sondhi, "A different view of the quantum hall plateau-to-plateau transitions," *Physical Review Letters*, vol. 79, no. 3, pp. 479–482, 1997.

[31] S. H. Pan, J. P. ONeal, R. L. Badzey et al., "Microscopic electronic inhomogeneity in the high-T superconductor Bi Sr CaCu O," *Nature (London)*, vol. 413, no. 6853, pp. 282–285, 2001.

[32] M. M. Qazilbash, A. Tripathi, A. A. Schafgans et al., "Nanoscale imaging of the electronic and structural transitions in vanadium dioxide," *Physical Review B*, vol. 83, no. 16, Article ID 165108, 2011.

[33] P. Dai, Y. Zhang, and M. P. Sarachik, "Low-temperature transport in the hopping regime: evidence for correlations due to exchange," *Physical Review Letters*, vol. 69, no. 12, pp. 1804–1806, 1992.

[34] H. Fritzsche and M. Cuevas, "Impurity conduction in transmutation-doped p-type germanium," *Physical Review*, vol. 119, no. 4, pp. 1238–1245, 1960.

[35] R. K. Ray and H. Y. Fan, "Impurity conduction in silicon," *Physical Review*, vol. 121, no. 3, pp. 768–779, 1961.

[36] M. Inada, H. Yamamoto, M. Gibo et al., "Crossover from Efros-Shklovskii variable range hopping to nearest-neighbor hopping in silicon nanocrystal random network," *Applied Physics Express*, vol. 8, no. 10, Article ID 105001, 2015.

[37] H. Fritzsche, "Electrical properties of germanium semiconductors at low temperatures," *Physical Review*, vol. 99, no. 2, pp. 406–419, 1955.

[38] A. S. Ioselevich, "Spin polarons and variable range hopping in magnetically disordered systems," *Physical Review Letters*, vol. 71, no. 7, pp. 1067–1070, 1993.

[39] J. H. Davies, "The density of states in the coulomb gap," *Philosophical Magazine B*, vol. 52, no. 3, pp. 511–520, 1985.

[40] M. Pollak, "The Coulomb gap: a review, and new developments," *Philosophical Magazine Part B*, vol. 65, no. 4, pp. 657–667, 1992.

[41] C. Yamanouchi, "Hall coefficient and resistivity in the intermediate impurity conduction of n-type germanium," *Journal of the Physical Society of Japan*, vol. 20, no. 6, pp. 1029–1034, 1965.

[42] H. Nishimura, "Impurity conduction in the intermediate concentration region," *Physical Review*, vol. 138, no. 3A, pp. A815–A821, 1965.

[43] E. M. Gershenzon, A. P. Mel'nikov, R. I. Rabinovich, and N. A. Serebryakova, "H⁻-like impurity centers and molecular complexes created by them in semiconductors," *Soviet Physics—Uspekhi*, vol. 23, no. 10, pp. 684–698, 1980.

[44] A. Kurobe and H. Kamimura, "Correlation effects on variable range hopping conduction and the magnetoresistance," *Journal of the Physical Society of Japan*, vol. 51, no. 6, pp. 1904–1913, 1982.

[45] T. G. Castner, N. K. Lee, G. S. Cieloszyk, and G. L. Salinger, "Dielectric anomaly and the metal-insulator transition in *n*-type silicon," *Physical Review Letters*, vol. 34, no. 26, pp. 1627–1630, 1975.

[46] A. Ferreira Da Silva, "Metal-insulator transitions in doped silicon and germanium," *Physical Review B*, vol. 37, no. 9, pp. 4799–4800, 1988.

[47] I. Terry, T. Penney, S. Von Molnr, and P. Becla, "Low-temperature transport properties of Cd0.91Mn0.09Te:In and evidence for a magnetic hard gap in the density of states," *Physical Review Letters*, vol. 69, no. 12, pp. 1800–1803, 1992.

[48] H. Vinzelberg, A. Heinrich, C. Gladun, and D. Elefant, "Activated conduction in Amorphous Cr-SiOx Thin films," *Philosophical Magazine B*, vol. 65, no. 4, pp. 651–656, 1992.

[49] R. W. van der Heijden, G. Chen, A. T. A. M. de Waele, H. M. Gijsman, and F. P. B. Tielen, "Simple activated transport in ion-implanted Si:As at temperatures below 0.5 K," *Solid State Communications*, vol. 78, no. 1, pp. 5–8, 1991.

[50] J.-J. Kim and H. J. Lee, "Observation of a nonmagnetic hard gap in amorphous In/InO$_x$ films in the hopping regime," *Physical Review Letters*, vol. 70, no. 18, pp. 2798–2801, 1993.

[51] V. Voegele, S. Kalbitzer, and K. Böhringer, "Observation of correlation effects in the hopping transport in amorphous silicon," *Philosophical Magazine B*, vol. 52, no. 2, pp. 153–168, 1985.

[52] K. G. Lisunov, E. K. Arushanov, C. Kloc, U. Malang, and E. Bucher, "Hopping conductivity in p-type β-FeSi2," *Physica Status Solidi (B) Basic Research*, vol. 195, no. 1, pp. 227–236, 1996.

[53] K. G. Lisunov, E. Arushanov, G. A. Thomas, E. Bucher, and J. H. Schön, "Variable-range hopping conductivity and magnetoresistance in n-CuGaSe2," *Journal of Applied Physics*, vol. 88, no. 7, pp. 4128–4134, 2000.

[54] A. Fedotov, S. Prischepa, A. Danilyuk, I. Svito, and P. Zukowski, "Spin-polarized and normal hopping magnetoresistance in heavily doped silicon," *Acta Physica Polonica A*, vol. 125, no. 6, pp. 1271–1274, 2014.

[55] K. A. Matveev, L. I. Glazman, P. Clarke, D. Ephron, and M. R. Beasley, "Theory of hopping magnetoresistance induced by Zeeman splitting," *Physical Review B*, vol. 52, no. 7, pp. 5289–5297, 1995.

[56] Y. Meir, "Universal spin-induced magnetoresistance in the variable-range hopping regime," *Europhysics Letters*, vol. 33, no. 6, pp. 471–476, 1996.

[57] S. V. Demishev and A. A. Pronin, "Magnetoresistance of carbon nanomaterials," *Physics of the Solid State*, vol. 48, no. 7, pp. 1363–1372, 2006.

[58] S. V. Demishev, A. D. Bozhko, V. V. Glushkov et al., "Scaling of magnetoresistance of carbon nanomaterials in Mott-type hopping conductivity region," *Physics of the Solid State*, vol. 50, no. 7, pp. 1386–1391, 2008.

[59] B. I. Shklovskiĭ and A. L. Éfros, "Percolation theory and conductivity of strongly inhomogeneous media," *Soviet Physics - Uspekhi*, vol. 18, no. 11, pp. 845–862, 1975.

[60] A. K. Fedotov, I. A. Svito, V. V. Fedotova, A. G. Trafimenko, A. L. Danilyuk, and S. L. Prischepa, "Low-temperature conductivity of silicon doped with antimony," *Semiconductors*, vol. 49, no. 6, pp. 705–711, 2015.

[61] B. Sandow, K. Gloos, R. Rentzsch, A. N. Ionov, and W. Schirmacher, "Electronic correlation effects and the Coulomb gap at finite temperature," *Physical Review Letters*, vol. 86, no. 9, pp. 1845–1848, 2001.

[62] I. Shlimak, M. Kaveh, R. Ussyshkin et al., "Temperature-induced smearing of the Coulomb gap: experiment and computer simulation," *Physical Review Letters*, vol. 75, no. 26, pp. 4764–4767, 1995.

[63] A. L. Danilyuk, A. G. Trafimenko, A. K. Fedotov, I. A. Svito, and S. L. Prischepa, "Negative differential resistance in n-type noncompensated silicon at low temperature," *Applied Physics Letters*, vol. 109, no. 22, Article ID 222104, 2016.

Composition Comments

1. Please check and confirm the author(s) first and last names and their order which exist in the last page.

2. We redrew Figure 6. Please check.

3. We made the highlighted change according to the list of references. Please check similar cases throughout.

4. We changed "ε" to "ϵ" in Figures 10 and 12 for the sake of consistency. Please check.

5. We incorporated reference [63] of the original manuscript within the text. Please check.

6. Comment on ref. [5]: Please provide the title of this reference.

Author(s) Name(s)

It is very important to confirm the author(s) last and first names in order to be displayed correctly on our website as well as in the indexing databases:

Author 1
Given Names: A. L.
Last Name: Danilyuk
Author 2
Given Names: A. G.
Last Name: Trafimenko
Author 3
Given Names: A. K.
Last Name: Fedotov
Author 4
Given Names: I. A.
Last Name: Svito
Author 5
Given Names: S. L.
Last Name: Prischepa

It is also very important for each author to provide an ORCID (Open Researcher and Contributor ID). ORCID aims to solve the name ambiguity problem in scholarly communications by creating a registry of persistent unique identifiers for individual researchers.

To register an ORCID, please go to the Account Update page (http://mts.hindawi.com/update/) in our Manuscript Tracking System and after you have logged in click on the ORCID link at the top of the page. This link will take you to the ORCID website where you will be able to create an account for yourself. Once you have done so, your new ORCID will be saved in our Manuscript Tracking System automatically.